Photocatalytic mechanism of metoprolol oxidation by photocatalysts TiO$_2$ and TiO$_2$ doped with 5% B: Primary active species and intermediates

Rodrigo Pereira Cavalcante [a], Renato Falcao Dantas [b], Bernardí Bayarri [c], Oscar González [c], Jaime Giménez [c,*], Santiago Esplugas [c], Amilcar Machulek Junior [a]

[a] Institute of Chemistry, Federal University of Mato Grosso do Sul, Av. Senador Filinto Muller, 1555, CP 549, CEP 79074-460 Campo Grande, MS, Brazil
[b] School of Technology, University of Campinas-UNICAMP, Paschoal Marmo 1888, Limeira, SP 13484-332, Brazil
[c] Department of Chemical Engineering, University of Barcelona, C/Martí i Franquès, 1, 08028 Barcelona, Spain

ABSTRACT

In photocatalysis, controversy still exists over as whether oxidation proceeds via primary oxidants, such as HO$^\bullet$ radicals, positive holes, electrons, O$_2{}^{\bullet-}$ radicals in the photodegradation process. The contribution of the main active species to the photocatalytic degradation of metoprolol (MET) using a solar simulator with Xenon lamp as irradiation source was examined by using different specific scavengers (formic acid, *tert*-butyl alcohol, ρ-benzoquinone and oxygen). According to this, we also compared the effect on the generation of active species, in the MET degradation, of two types of TiO$_2$ catalyst having different physical and chemical properties: pure TiO$_2$ and TiO$_2$ doped with 5% B (w/w), both synthesized by sol-gel method. The scavenger study indicates that HO$^\bullet$ radicals are the dominant reactive species, contributing around 80% and to a lesser extent by the contribution of O$_2{}^{\bullet-}$ radicals and holes in systems using TiO$_2$ doped with 5% B (w/w). However, when pure TiO$_2$ was used as catalyst, experiments carried out in ρ-benzoquinone demonstrate that O$_2{}^{\bullet-}$ radicals did not participate in the degradation mechanism of MET. Oxygen seems to play an important role during the observed degradation of MET. Additionally, the relation between the intermediates formed during the photocatalytic degradation with TiO$_2$ doped 5% B (w/w) as catalyst, with addition of specific scavengers, was investigated and distinct degradation pathways have been proposed for each active species involved. By-products studies in the presence of scavengers were used as a diagnostic tool for the analysis of the photocatalytic mechanism and it was possible to prove that there is change in the reactions of the degradation process of MET when change the role of any active species generated on the surface of the catalyst.

© 2016 Elsevier B.V. All rights reserved.

1. Introduction

Heterogeneous photocatalysis, as a method to degrade organic contaminants, has been a subject of great interest, forming part of a group of processes known as Advanced Oxidation Processes (AOPs) [1,2]. This technique is effective for water treatment because of a number of important characteristics, such as: (1) low costs; (2) operation at mild condition of temperature and pressure; (3) unlike conventional treatment, which transfer pollutants from one medium to another, photocatalysis can easily degrade and even mineralize almost all the organic compounds; (4) the reaction time

is reasonable and a lesser chemical input is required; (5) it can be applied to aqueous systems, as well as solid- (soil-) and gas phase systems [1,3–7].

Among many semiconductor photocatalysts (including TiO$_2$, ZnO, SnO$_2$, WO$_3$, ZnS, PbS, CdS, CdSe, Fe$_2$O$_3$, Cu$_2$O), TiO$_2$ is considered as the best known semiconductor for photocatalysis due several aspects. For example, it is highly active, chemically stable in solution over a wide pH range, cheap, readily available material, not subject to photocorrosion, and, in addition, it has low toxicity and, relatively low selectivity [8–13].

When TiO$_2$ is excited with a photon with energy equal or higher than its bandgap (3.2 eV for anatase and 3.0 eV for rutile) electron–hole pairs Eq. (1) are produced in the conduction and valence band, respectively [2,14]. These electrons and holes migrate to the surface of the semiconductor, where they either recombines,
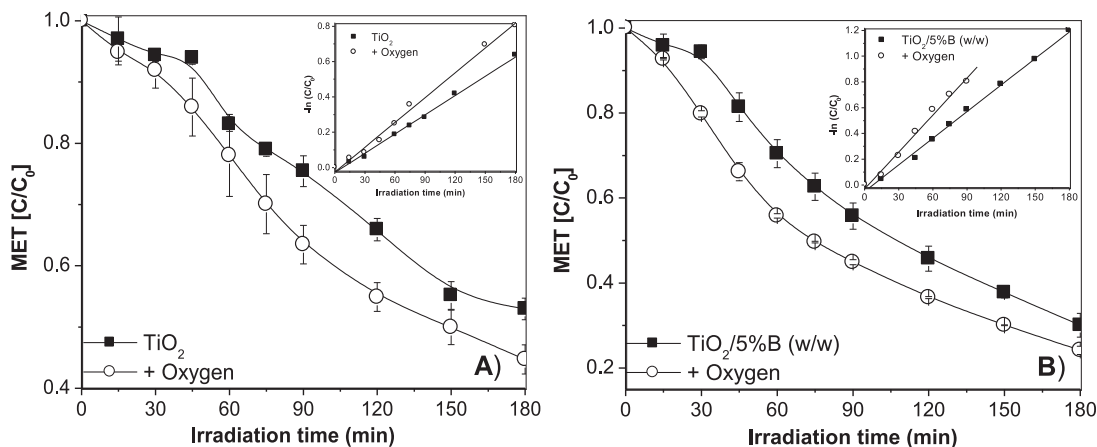
Fig. 1. Effect of the oxygen dissolved on the efficiency of photocatalytic degradation of MET for pure TiO_2 (A) and 5% B (w/w) doped TiO_2 (B). $[MET]_0 = 50\,mg\,L^{-1}$, [catalyst] $= 0.4\,g\,L^{-1}$.
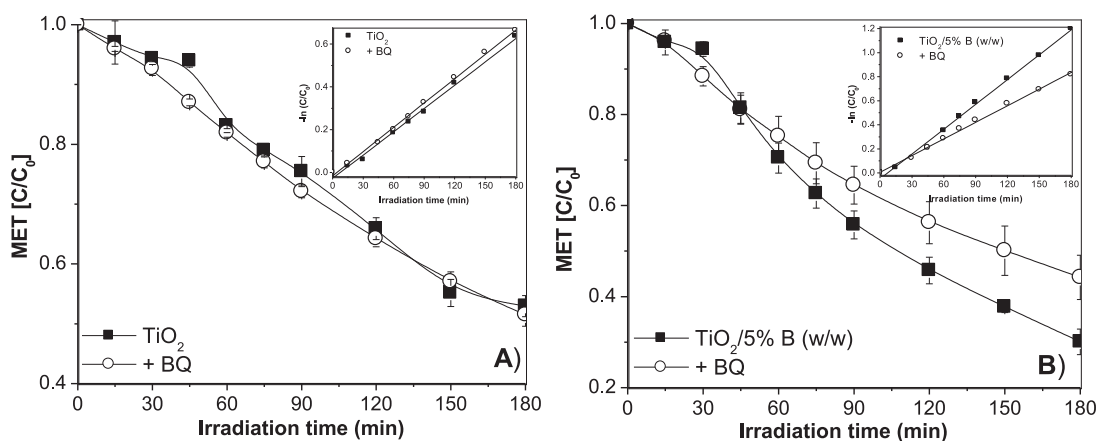

Fig. 2. Effect of the ρ-benzoquinone addition on the photocatalytic degradation of MET for pure TiO_2 (A) and 5% B (w/w) doped TiO_2 (B). $[MET]_0 = 50\,mg\,L^{-1}$, [catalyst] $= 0.4\,g\,L^{-1}$.
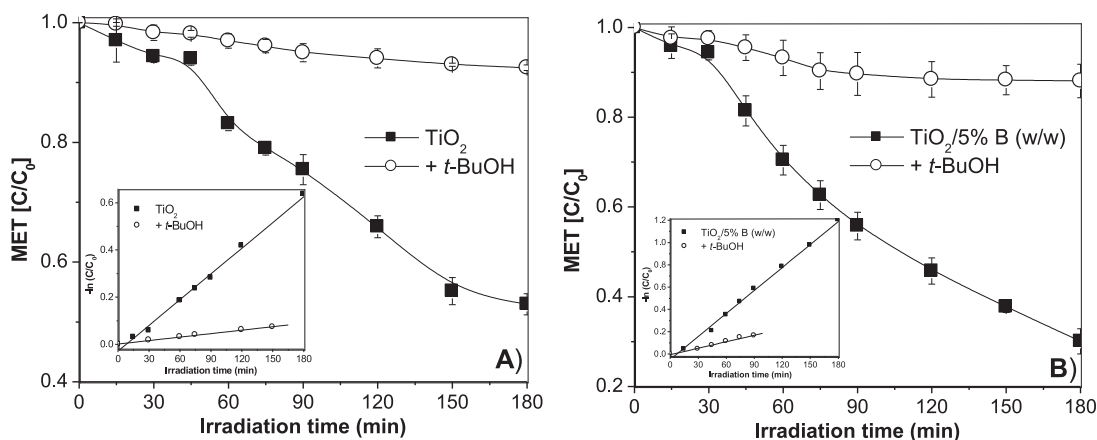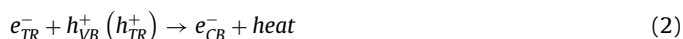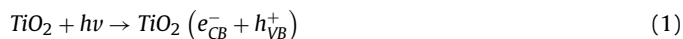

Fig. 3. Effect of *tert*-butyl alcohol addition on the photocatalytic degradation of MET for pure TiO_2 (A) and 5% B (w/w) doped TiO_2 (B). $[MET]_0 = 50\,mg\,L^{-1}$, [catalyst] $= 0.4\,g\,L^{-1}$.

liberating heat Eq. (2), and/or participate in redox reactions with species adsorbed on the photocatalyst Eqs. (3–6) [9,15]. The positive hole produced may reacts with water and hydroxide ion to produce hydroxyl radicals, HO• (adsorbed and free, Eqs. (3) and (4)) or directly oxidizes pollutants (Eq. (5)) [5,13]. Similarly the electron can be donated to an electron acceptor (oxygen adsorbed) to produce superoxide radical anion, $O_2^{\bullet-}$ Eq. (6) [2,5]. This $O_2^{\bullet-}$ radical then may react with proton forming perhydroxyl radical

($HO_2^\bullet$) and subsequently H_2O_2 that may then be reduced to HO• radicals [3,9,16,17].

$$TiO_2 + h\nu \rightarrow TiO_2\left(e_{CB}^- + h_{VB}^+\right) \tag{1}$$

$$e_{TR}^- + h_{VB}^+\left(h_{TR}^+\right) \rightarrow e_{CB}^- + heat \tag{2}$$

$$h_{VB}^+ + H_2O \rightarrow HO_{free}^\bullet + H^+ \tag{3}$$

$$h_{VB}^+ + HO_{ads}^- \rightarrow HO_{ads}^\bullet \tag{4}$$

$$h_{VB}^+ + R \rightarrow R^{\bullet +} \qquad (5)$$

$$e_{CB}^- + O_2 \rightarrow O_2^{\bullet -} \qquad (6)$$

Essentially, these reactive transitory species generated (HO$^\bullet$, O$_2$$^{\bullet -}$, h$_{VB}$$^+$, HO$_2$$^\bullet$) are the main responsible for the degradation of organic pollutants present in the medium. However, one of the questions raised in discussions on photocatalysis concerns the role of the oxidizing species involved in photoreaction process [16,18,19].

The HO$^\bullet$ radicals are often assumed as the major reactive species responsible for the degradation of organic molecules. This is supported by the experimental observation of a large number of hydroxylated intermediates detected during the photocatalytic degradation of aromatic contaminants, distribution of the hydroxylation products, and spin trapping with subsequent electronic spin resonance (ESR) detection [18,20].

Many studies have been devoted to understand the mechanism of the oxidizing species generated in the interface of the catalyst under irradiation, which is essential for understanding the mechanism of photocatalytic reaction [16]. To help on this type of investigation, several substances, called scavengers, whose purpose is to alter the kinetic profile of organic compounds oxidation, have been used to elucidate the role of the different active species present in the degradation process [21].

Although many researchers have paid attention to the use of different scavengers in photocatalytic reactions [16,21–25], their fundamental aims were investigate the participation of the different active species present in the process. Thus, in the photocatalytic system, the identification of the different generated active species is important, nevertheless it is more important to distinguish the roles of each active species on degradation reaction pathways.

Over the last years, pharmaceuticals have been receiving increasing attention of the scientific community as potencial micropollutants in aquatic environments [26]. These contaminants may affect water quality and potentially impact drinking water supplies, ecosystem and human health [27].

One of the classes of pharmaceuticals more consumed by the world population are β-blockers, therefore they are considered emerging contaminants [28].

These drugs are used for the treatment of different cardiovascular diseases, such as high blood pressure (hypertension), coronary artery disease and arrhythmias [29,30].

As β-blockers are widely used, not only in hospitals but also domestically, their presence use has been continually measured in wastewater treatment plants (WWTP), hospital wastewater (HWW) and surface water at concentrations in the order of ng L^{-1} to µg L^{-1} [28,31].

In a previous work [32] we studied the use of TiO$_2$ doped with 5% B (w/w) to remove MET in ultrapure water and municipal secondary effluent under simulated sunlight. The results clearly indicate that the TiO$_2$ doped with 5% B treatment can efficiently eliminate MET from both water matrix. A substantial improvement of biodegradability was also achieved and no toxic products were formed at the end of the process. The results also showed that the decrease in MET concentration led to the formation of a number of organic intermediates and MET degradation pathway was proposed. The catalyst was previously prepared in our laboratories and characterized by different techniques [33].

Despite the role of active species in the mechanisms in the photocatalytic process has being investigated by many research groups, the role that active species play in the degradation of organic substances remain still obscure and controversial, because it depends on the substrate type and catalyst structure [21,34,35]. In this context, the aim of this work has been to understand the contribution of main active species in the photodegradation of MET using pure TiO$_2$ and TiO$_2$ doped with 5% B (w/w) through the use of specific scavengers for holes, radicals, and electron. Additionally, the relation between the intermediates formed during the photocatalytic degradation and actives species was discussed using the qualitative analysis of the intermediates and degradation pathway in the presence and/or absence of scavengers.

2. Materials and methods

2.1. Chemicals

All chemicals were of analytical grade. Metoprolol tartrate salt (MET, purity >99%) (CAS n° 56392-17-7/(C$_{15}$H$_{25}$NO$_3$)$_2$C$_4$H$_6$O$_6$, MW 684.81 g mol^{-1}) was purchased from Sigma Aldrich Chemical Co. Formic acid (85%), *tert*-butyl alcohol (99.7%) and ρ-benzoquinone (>99%) were purchased from Probus S.A. (Spain), Panreac (Spain) and Merck (Germany), respectively. Acetonitrile, used as mobile phase for HPLC, was purchased from Fisher Chemical. Other chemicals and solvents were purchased from various commercial suppliers and used as received. The used filters were Millipore Millex syringe-driven 0.45-µm (pore size) polyethersulfone membrane filters. Deionized water was produced in a Direct-Q Millipore and was used in all experiments.

The investigated photocatalysts were pure TiO$_2$ and TiO$_2$ doped with 5% B (w/w), synthesized by means of the sol–gel method [33]. The main characteristics of these TiO$_2$ powders are listed in Table 1.

2.2. Experimental set up

The experiments were carried out in a solar simulator (Solarbox, Co.fo.me.gra, 220 V, 50 Hz) equipped with a Xenon lamp (Phillips XOP 1 kW) and an optical filter (cut-off <280 nm) located just below the lamp. The procedure was as follows: A stirred reservoir tank (total volume 1 L) was filled with MET aqueous solution following the addition of 0.4 g L^{-1} of catalyst and different scavengers when needed. The aqueous suspension was continuously pumped with a flow rate of 0.65 L min^{-1} (peristaltic pump Ecoline VC-280 II, Ismatec) into the Duran tubular photoreactor (24 cm length, 2.11 cm diameter, 0.078 L illuminated volume) placed at the bottom of the solar simulator in the axis of a parabolic mirror made of aluminum reflective material inside of the chamber. The photon flux inside the photoreactor was 2.99 × 10^{-6} Einstein s^{-1} (290–400 nm), determined by *o*-nitrobenzaldehyde (o-NB) actinometry [36]. To keep the solution at 25 °C, the jacket temperature of the stirred tank was controlled with a thermostatic bath (Haake K10).

2.3. Effect of radical inhibitors

In order to capture reactive species during the photocatalytic reactions, formic acid (FA), *tert*-butyl alcohol (*t*-BuOH), oxygen and/or ρ-benzoquinone (BQ) were added to the MET solutions containing catalyst, for the elucidation of the role of the different species associated with degradation and its intermediaries. The study was conducted using a suitable amount of each sequestering compound: oxygen (saturation with air); BQ (0.0080 g L^{-1} corresponding to a molar relation of 1:10 for BQ:MET); 1.0 g L^{-1} FA; or 60 mL L^{-1} *t*-BuOH. These concentrations were based on previous studies [36].

2.4. Analytical procedures

MET degradation was monitored by HPLC (1200 Infinity Series from Agilent) under the following conditions: C18 reverse phase column (SEA18 5 µm 15 × 0.46 cm from Teknokroma), water and acetonitrile (78:22) as the mobile phase, injected with a flow-rate of 0.850 mL min^{-1}, and a Waters 996 photodiode array detector
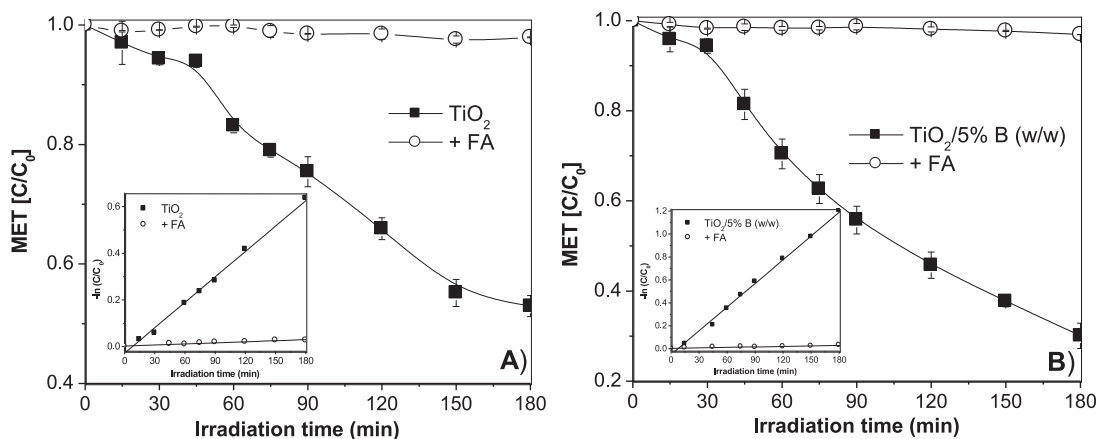
Fig. 4. Effect of formic acid addition on the photocatalytic degradation of MET for pure TiO_2 (A) and 5% B (w/w) doped TiO_2 (B). $[MET]_0 = 50\,mg\,L^{-1}$, $[catalyst] = 0.4\,g\,L^{-1}$.

Fig. 5. Proposed pathways for the photocatalytic degradation of MET by TiO_2/5% B (w/w) catalyst in aqueous solution saturated with air.

Table 1
Characteristics of the catalysts [33].

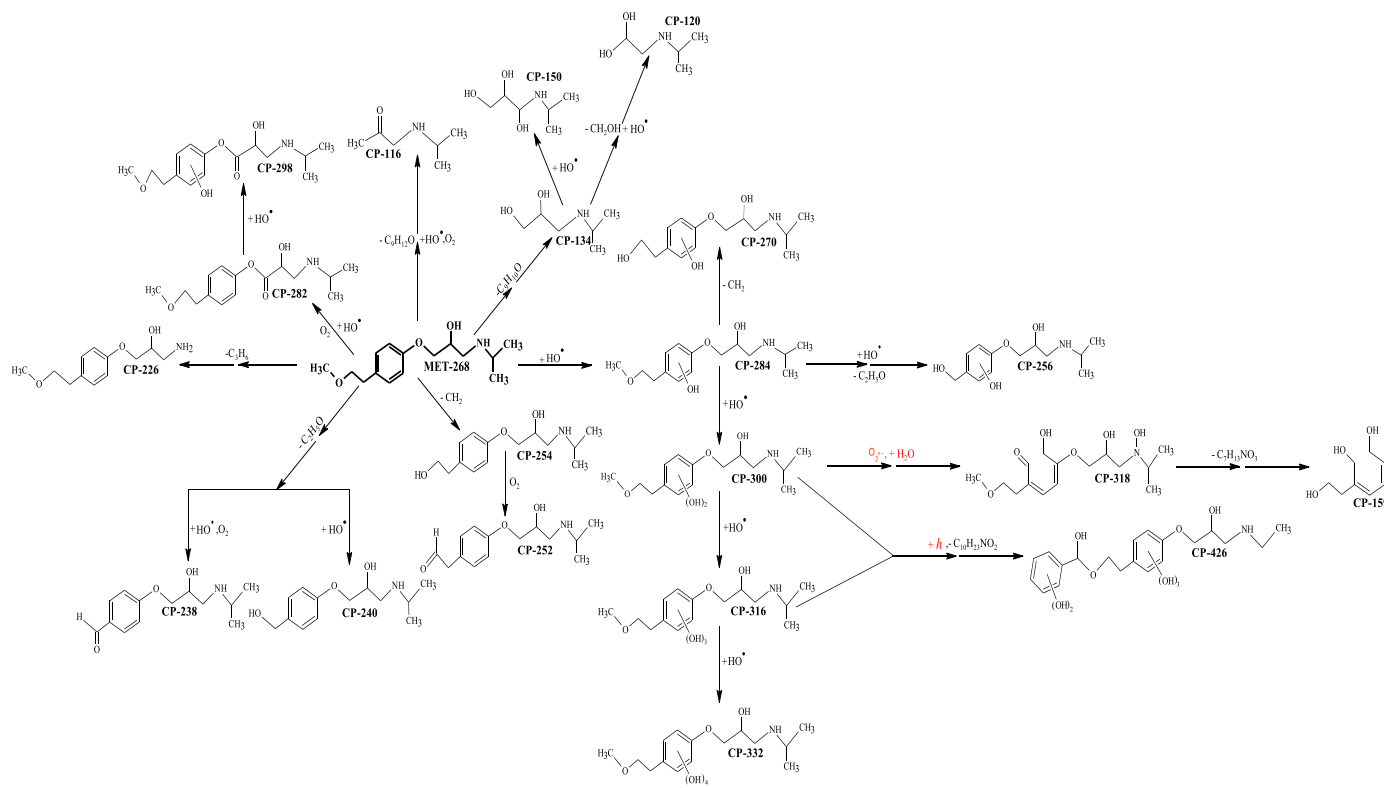| Catalyst	Surface area (m^2/g)	Crystalline form	Anatase crystallite size (nm)	Bandgap energy (eV)	Particle size (nm)
TiO_2	~68	Anatase (100%)	28.49	3.05	21.29
TiO_2-5% B	~100	Anatase (74%)/rutile (26%)	16.59	3.04	10.54

Fig. 6. Proposed pathways for the photocatalytic degradation of MET by TiO$_2$/5% B (w/w) catalyst in the presence of prominent HO$^\bullet$ radicals and holes.

using the Empower Pro software 2002 Water Co., working at maximum UV absorbance (221.9 nm). In order to remove the catalyst, before the analysis, samples were filtered with a polyethersulfone membrane filter of 0.45 μm.

For the intermediates identification, samples were analyzed by HPLC (Agilent Series 1100) under the same conditions used previously for monitoring degradation of MET. The HPLC system is connected to LC/MSD-TOF (Agilent Technologies) mass spectrometer operated in the positive electrospray ionization mode (ESI–MS) and using the following parameters: capillary 4000 V; nebulizer 15 psig; drying gas, 7 L min^{-1}; gas temperature, 325 °C; fragmentator, 175 V. Spectra were acquired over the m/z 60–1200 range.

3. Results and discussion

3.1. Contribution of the active species to the photodegradation rate of MET

First, the roles of the main active species, such as holes, electrons, O$_2^{\bullet-}$ and HO$^\bullet$ radicals were investigated using the different scavengers.

3.1.1. Effect of the presence of an electron acceptor: oxygen

Electron/hole (e$_{BC}^-$/h$_{BV}^+$) recombination is one of the crucial reaction in the application of TiO$_2$ as photocatalyst, and it is well known and discussed that the use of electron acceptors, such as oxygen, can inhibit strongly this recombination and consequently improve the photocatalytic activity [37,38].

In order to evaluate the role of dissolved oxygen on the rate of the MET photocatalytic degradation, during all the experiment time the solution was saturated with oxygen by continuously bubbling synthetic air with the aid of gas diffusers. Before all experiments, the solution was purged continuously with atmospheric air for at least 20 min in the dark to ensure that the level of oxygen saturation is reached and to nullify the effect of adsorption.

The results presented in Fig. 1A and B show that an excess of oxygen has a beneficial effect on degradation (e.g. 9% and 17% of increase in the degradation of MET after 180 min is observed when applying air using TiO$_2$ doped 5% B and pure TiO$_2$ as catalysts, respectively).

These results were corroborated with higher values of the pseudo-first order kinetic constant (k$_{ap}$) obtained in experiments with O$_2$. k$_{ap}$ values could be obtained from the regression line slopes representing −ln (C/Co) vs. time of irradiation. The fitted curve of −ln (C/Co) vs. time is presented in the inset of Fig. 1A and B for both catalysts used. The obtained pseudo-first-order rate constants with or without scavengers and the corresponding regression coefficients are all summarized in Table S1 (Supplementary material).

The value of k$_{ap}$ in the presence of oxygen increases from 3.63×10^{-3} min^{-1} to 4.69×10^{-3} min^{-1} using pure TiO$_2$ and from 6.88×10^{-3} min^{-1} to 9.55×10^{-3} min^{-1} using TiO$_2$ doped 5% B. This verifies that O$_2$ plays a key role in the photocatalytic degradation of MET, as is noticed during the degradation of other organic compounds using heterogeneous photocatalysis [22,39,40].

Oxygen adsorbed on the TiO$_2$ surface prevents the recombination of e$^-$/h$^+$ pairs by trapping electrons with the formation of O$_2^{\bullet-}$ radicals [16] which lead to increase lifetime of holes, thus promoting the formation of more HO$^\bullet$ radicals [38,40]. Additionally, the O$_2^{\bullet-}$ radicals have the potential to react directly by oxidative pathways, forming singlet oxygen or decomposing to H$_2$O$_2$, which is transformed in more HO$^\bullet$ radicals [38,40].

In addition to these factors listed above that are responsible for improving photocatalysis in the presence of oxygen, it can also be highlighted the increased oxidation rate of intermediate compounds (see Fig. 5 and Table S2 of Supplementary material) and the reduction of problems caused by low molecular oxygen concentration can also be highlighted [16,37,41].
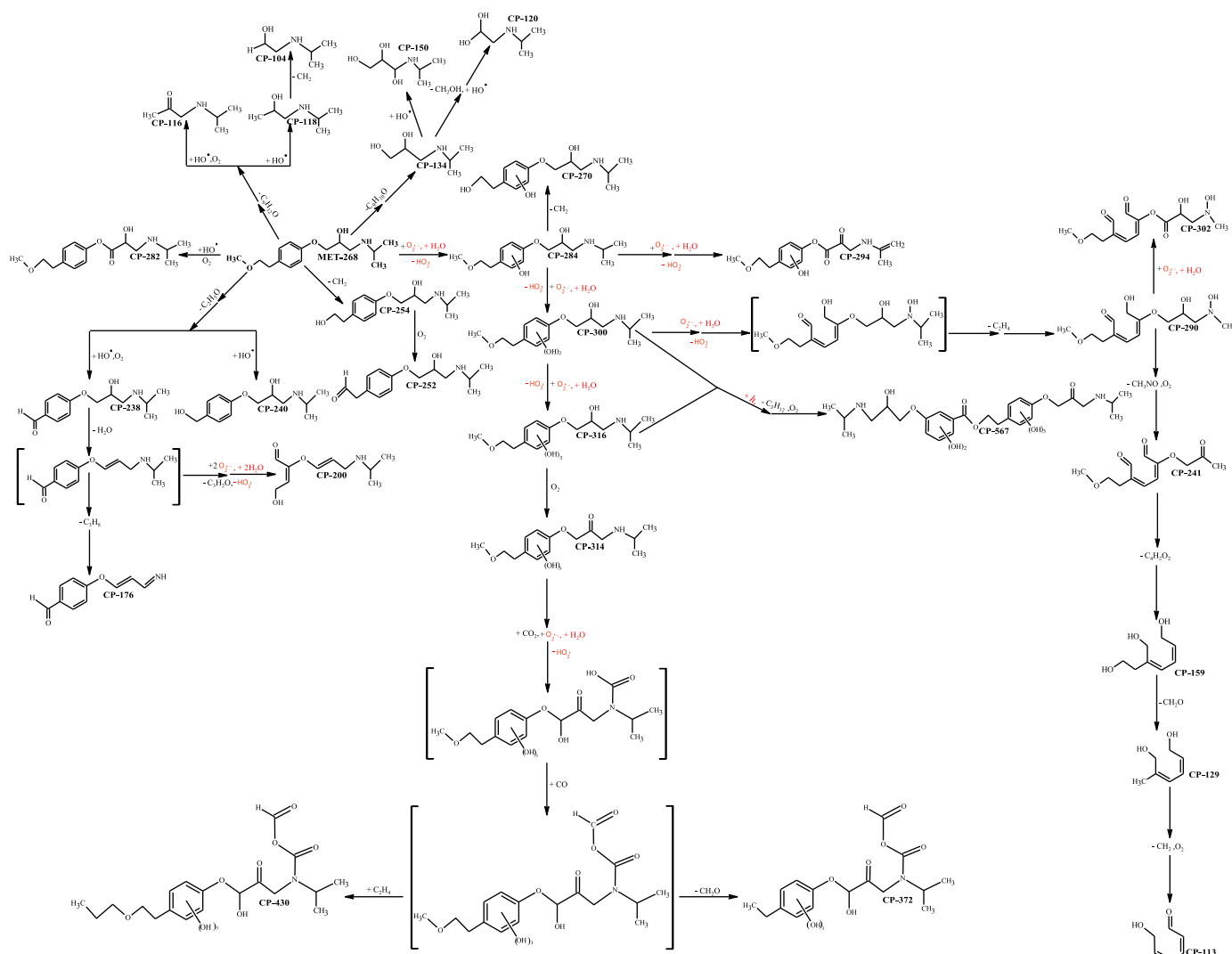
Fig. 7. Proposed pathways for the photocatalytic degradation of MET by $TiO_2/5\%$ B (w/w) catalyst in the presence of prominent $O_2^{\bullet-}$ radicals and holes.
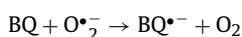
Thus, the O_2 saturation proves to be necessary to increases the efficiency of photocatalytic degradation reactions.

3.1.2. Effect of the presence of superoxide radical anion scavengers: ρ-benzoquinone (BQ)

The superoxide radical anion ($O_2^{\bullet-}$) is produced by the reduction of oxygen molecules adsorbed on the catalyst surface by the photogenerated electrons [21]. Studies have shown [42] that this active species plays more important role than $HO^{\bullet}$ radicals in the photocatalytic reaction for E. coli inactivation by use of natural magnetic sphalerite as catalyst. This demonstrates the importance of investigate this reactive oxygen species in studies of photocatalysis.
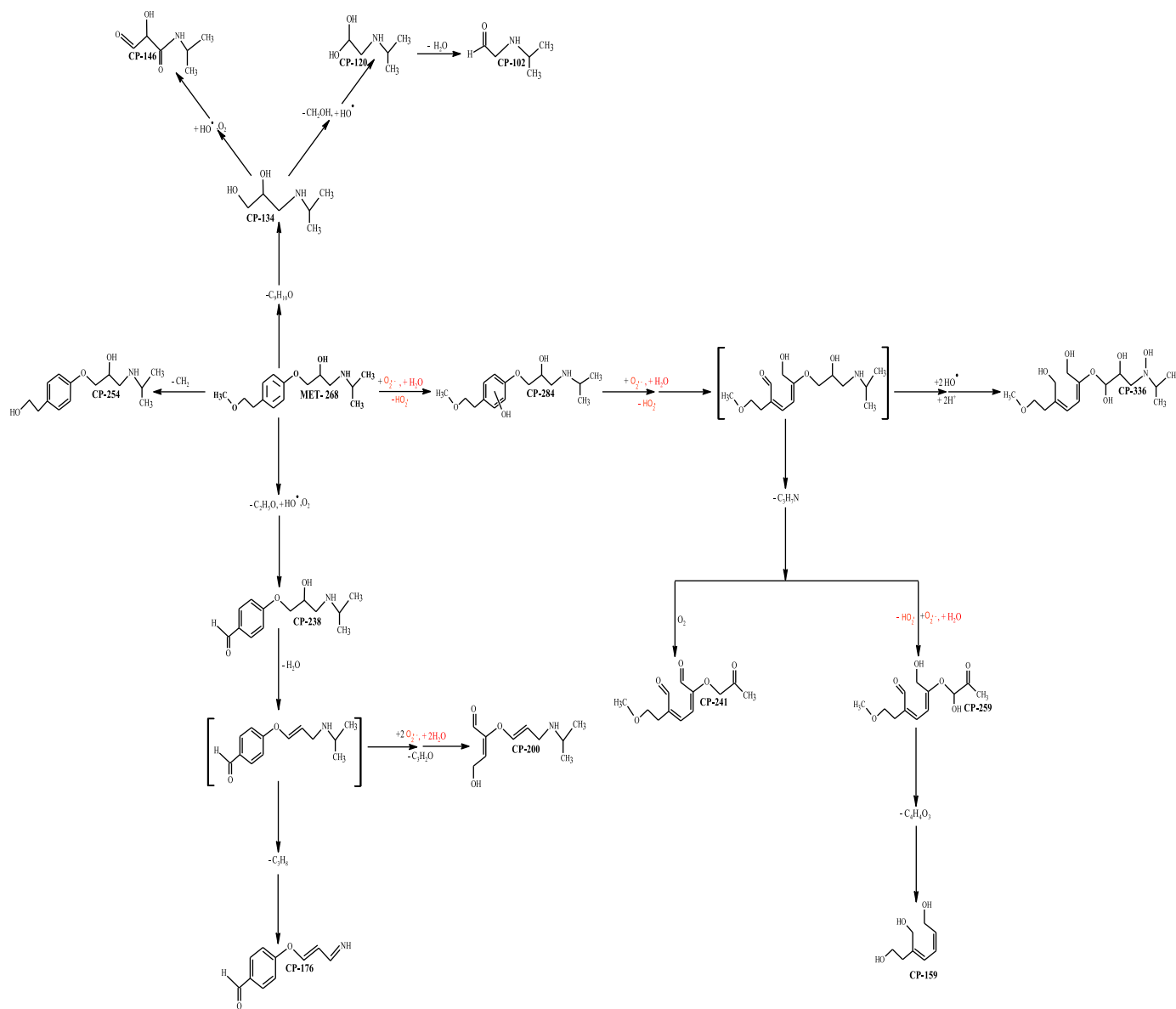
BQ has been used by various researchers to verify the involvement of $O_2^{\bullet-}$ radicals on the photocatalytic degradation of various organic compounds in water [21,23,34,36,43,44].

In order to determine the participation of $O_2^{\bullet-}$ radicals in the process, BQ was added (Fig. 2A and B). BQ can be used to detect the O_2^- radicals due to their ability to trap this anion radical by a simple electron transfer mechanism, according to Eq. (7), [36,43] with a rate constant value of 0.9–1.0×10^9 M^{-1} s^{-1} [45].

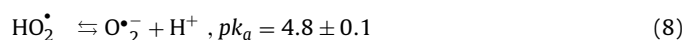$$BQ + O_2^{\bullet-} \rightarrow BQ^{\bullet-} + O_2 \qquad (7)$$

The addition of BQ provokes partial inhibition of the MET degradation (about 20% inhibition) using TiO_2 doped with 5% B (w/w) as shown in Fig. 2B. The degradation rate also was largely suppressed and k_{ap} constants decrease from 6.88×10^{-3} min^{-1}, in the absence of scavenger, to 4.61×10^{-3} min^{-1} in the presence of BQ (Table S1 in Supplementary material). However, under the same experimental conditions, but with pure TiO_2, no inhibition was observed in the presence of BQ.

The O_2^- radical is always in equilibrium with its conjugate acid, the perhydroxyl radical, $HO_2^{\bullet}$ Eq. (8) [46]. The results of catalysts characterization [33] verify that the point of zero charge (pzc) of the TiO_2 doped with 5% B (w/w) occurs at pH 5.34. Thus, the surface of the $TiO_2/5\%$ B (w/w) may be positively charged at pH <5.34 and negatively charged at pH >5.34. Since the pKa value of the equilibrium among these species ($HO_2^{\bullet} \leftrightarrows O_2^{\bullet-}$) is 4.8 ± 0.1 [46,47], the $O_2^{\bullet-}$ radicals become the predominant species in solution at pH 6.0 [48], with this we can conclude that superoxide radicals are the predominant species in solution using $TiO_2/5\%$ B (w/w) as catalyst, since the experiments were performed in pH 6.3 with this catalyst. For pure TiO_2 the pzc occurs at pH 4.24 [33]. This can change the balance of Eq. (8) and the formation of $HO_2^{\bullet}$ radicals are probably favored, since the $O_2^{\bullet-}$ radicals are few protonated at this pH. Therefore, for pure TiO_2 the formed species are $HO_2^{\bullet}$ radicals. This probably explains the no contribution of $O_2^{\bullet-}$ radicals in pure TiO_2. Chen

Fig. 8. Proposed pathways for the photocatalytic degradation of MET by TiO$_2$/5% B (w/w) catalyst in the presence of prominent O$_2$$^{\bullet-}$ radicals.

et al. [49] demonstrated in their study that the O$_2$$^{\bullet-}$ radicals does not participate in the reaction for destruction of bacterial cells using natural semiconducting mineral sphalerite, as catalyst. Fang et al. [50] also demonstrated that HO$^{\bullet}$ radicals were the most important reactive oxygen species mediating photocatalytic degradation of propylparaben preservative in aqueous suspension of P25 TiO$_2$. In this case, the results indicate that h^{+} was not remarkable due to low adsorptive capacity of propylparaben and a smaller contribution was associated to indirect degradation of reductive species e^{-} which produced various oxidative species, such as O$_2$$^{-}$ radicals at TiO$_2$ conduction band. Nevertheless, the contribution of each active species is dependent on the organics, as well as the catalyst.

$$HO_2^{\bullet} \leftrightarrows O_2^{\bullet-} + H^{+} \, , \, pk_a = 4.8 \pm 0.1 \qquad (8)$$

3.1.3. Effect of the presence of hydroxyl radical scavengers:tert-butyl alcohol (t-BuOH)

The effect of alcohols, such as methanol, isopropanol and *t*-BuOH, on the photocatalytic degradation rate has been commonly used as tool for the diagnostic for HO$^{\bullet}$ free-mediated mechanisms [20,51,52].

Though direct oxidation of short aliphatic alcohols by photogenerated holes probably occurred, it can be considered as negligible because they have a very weak adsorption on TiO$_2$ surface in aqueous media. Thus, alcohols are usually used as diagnostic tools of HO$^{\bullet}$ radicals [16,20,22,51–53].

The *t*-BuOH, is considered an excellent capturer of HO$^{\bullet}$ radicals, reacting as illustrated by Eq. (9) [36,40], with a reaction rate constant of 6.0 × 10^{8} M^{-1} s^{-1} [54–56]. *t*-BuOH reacts with HO$^{\bullet}$ radicals, generating inert intermediates, thus causing termination of the radical chain reactions. Therefore, *t*-BuOH is a more suitable indicator for the HO$^{\bullet}$ radical type reaction [57].

$$HO + t - BuOH \rightarrow (CH_2C(CH_3)_2OH) + H_2O \qquad (9)$$
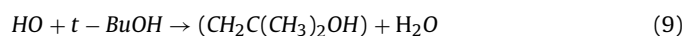
In Fig. 3A and B it can be seen that the presence of *t*-BuOH has a very strong influence on the degradation of MET, leading to over 80% inhibition after 180 min of irradiation for both catalysts and, consequently, causing a drastic reduction in the degradation rate (see Table S1 in Supplementary material). This suggests that free HO$^{\bullet}$ radicals play an important role in the photocatalytic degradation of MET in both pure or 5% B (w/w) doped TiO$_2$.
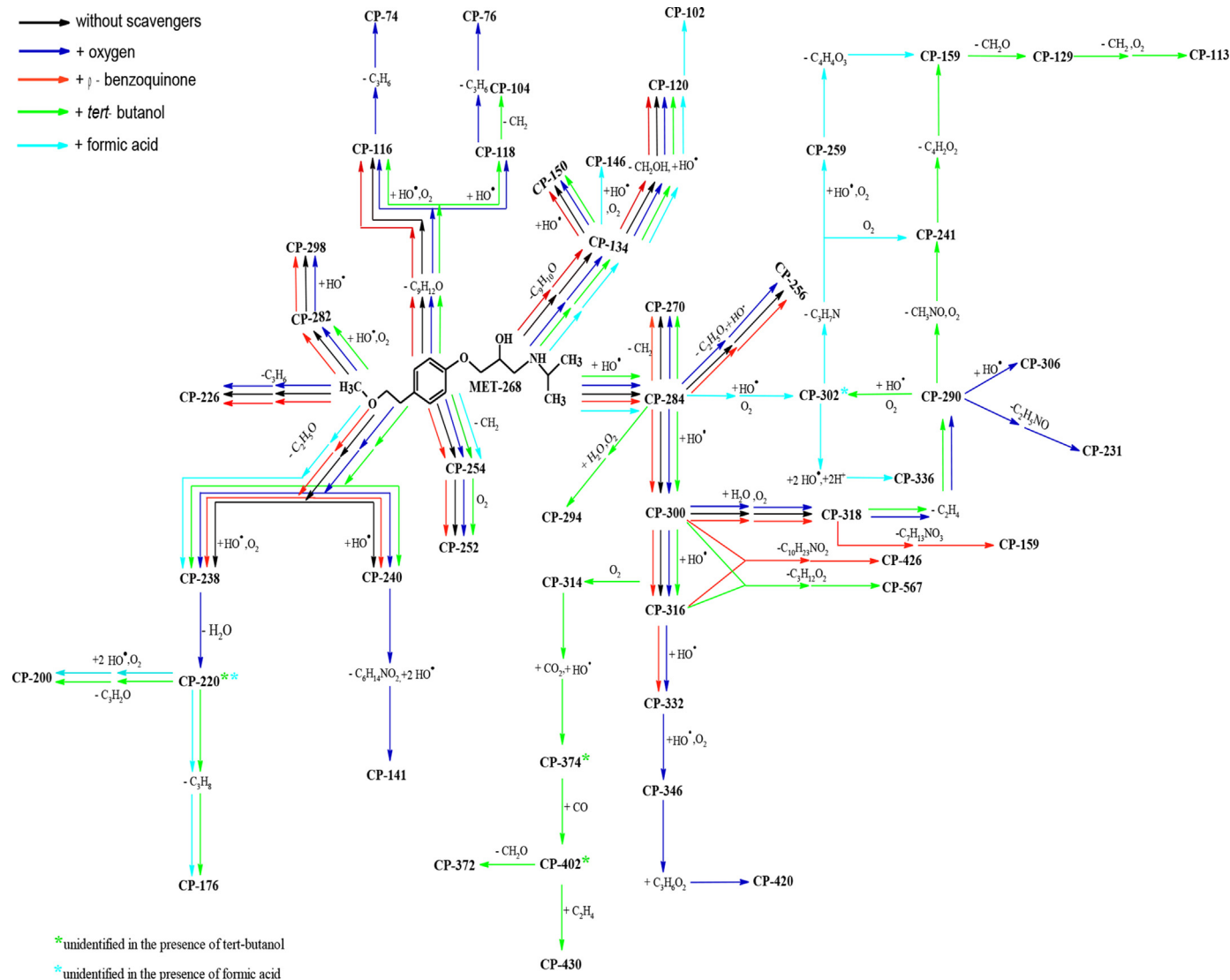
Fig. 9. Comparison of different proposed pathways for the photocatalytic degradation of MET by TiO₂/5% B (w/w) catalyst in the absence and presence of scavengers specific.

3.1.4. Effect of holes scavengers: formic acid (FA)

The participation of the holes in the photocatalytic reaction can be assessed with the use of the FA [36,40,58–61]. The FA oxidation to carbon dioxide is straight forward and involves minimal intermediate products [60].

This scavenger consumes the holes by $HCOO^-$ (as demonstrated by Eq. (10)) which in addition can eliminate or intercept the generation of $HO^\bullet$ radicals (Eq. (11)) on TiO₂ surface [36,59,61]. FA under neutral and acidic conditions is strongly adsorbed onto the surface of TiO₂ [36,40].

$$HCOO^- + 2h^+ \rightarrow CO_2 + H^+ \tag{10}$$

$$HCOO^- + HO \rightarrow CO_2^- + H_2O \tag{11}$$

When FA was introduced into the solution as diagnostic tool for suppressing the holes process, the photocatalytic degradation of MET was completely inhibited for both catalysts, as shown in Fig. 4A and B. This occurs because the acid is used to evaluate the contribution of both species, positive holes and HO• radicals (free and adsorbed). Knowing that t-BuOH scavenges free HO• radicals and AF both holes and HO• radicals, it can be assumed that the greater the inhibition of the reaction by AF in comparison to inhibition by

t-BuOH, most direct participation of the holes in the photocatalytic degradation of MET.

3.1.5. Estimated contribution of each active species in the MET degradation

Relevant contributions for the different active species during the photocatalytic degradation of MET at different scavengers for both catalysts are presented in Table 2. Knowing that AF scavenges both, holes and HO• radicals, one can calculate the minimum percentage of holes and free HO• radicals which participate in the photocatalytic degradation of MET, as well as of $O_2^{\bullet-}$ radicals. The difference between the percentages of inhibition of MET degradation and the addition of t-BuOH and AF results in the direct contribution of the holes and adsorbed HO•.

On the basis of data obtained, everything seems to indicate that more than 80% MET degradation was achieved via oxidation of free HO• radicals for both catalysts analyzed, indicating that this is major active species participating on the degradation process. Similar results have been reported in previous studies [35]. The results obtained by An et al. [35], for antivirus drug acyclovir in P25 TiO₂ suspension showed that the drug oxidation was driven mainly by the participation of HO• radicals. $O_2^{\bullet-}$ radicals produced by photoexcited electrons and photogenerated holes on the cata-

Table 2
Percentage of inhibition due to the scavengers, and the percentage of contribution of each active species during the photocatalytic degradation of MET using pure TiO_2 and TiO_2 doped with 5% B (w/w) as catalysts. $[MET]_0 = 50\,mg\,L^{-1}$, $[catalyst] = 0.4\,g\,L^{-1}$.

Catalyst	Percentage of inhibition			Percentage of contribution		
	t-BuOH (%)	AF (%)	BQ (%)	$HO^{\bullet}_{free}$ (%)	h^+ (%)	$O_2^{\bullet-}$ (%)
TiO_2	84.0 ± 0.99	94.3 ± 2.32	0.00	84.0 ± 0.99	10.3	0.00
TiO_2/5% B	82.9 ± 7.52	95.6 ± 0.007	20.3 ± 9.76	82.9 ± 7.52	12.7	9.85 ± 5.05

lyst surface also participate on the degradation process using TiO_2 doped with 5% B. However, $O_2^{\bullet-}$ radicals did not play role in the MET degradation process using pure TiO_2 as catalyst. These results confirmed that roles of the active species are different in different degradation systems and depend on the substrate structure (see Table 1), as previously mentioned by Palominos et al., Li et al., and An et al. [21,34,35].

If 100% is the total amount of active species present in the medium, Table 2 shows values slightly exceeding 100% for the catalyst doped with 5% B (w/w). The BQ also has the ability to react with the $HO^{\bullet}$ radicals with rate constant equal to $6.9 \times 10^5\,s^{-1}$ at pH 6.2 [45,62]. The results of catalysts characterization [33] verify that the point of zero charge of the catalyst doped with 5% B (w/w) occurs at pH 5.34. Thus, for this catalyst, $HO^{\bullet}$ radicals can be more easily eliminated by BQ. However for pure TiO_2 suspension the point of zero charge occurs at pH 4.24. Since the value of rate constant decreases at low pH values [62], it can be concluded that the reaction rate of $HO^{\bullet}$ radical with BQ for this catalyst is low. This probably explains the values slightly exceeding 100% of percentage of contribution of each active species during the photocatalytic degradation for TiO_2/5% B (w/w) catalyst. However, it was possible to estimate with confidence the participation of the main active species in the MET degradation.

In the following part, we further investigate the relationship among these active species and the intermediates formed in the degradation of MET by TiO_2 doped with 5% B.

3.2. Relationship between the active species and the intermediates formed in MET degradation

The LC/MS technique was used to probe the main by-products of MET (experiment with $50\,mg\,L^{-1}$ MET, $0.4\,g\,L^{-1}$ TiO_2 doped with 5% B (w/w) in the presence of the different scavengers (Oxygen, BQ, t-BuOH and AF)) obtained at 90 min and 180 min of photocatalytic degradation. The masses of the different products were determined from the peaks corresponding to the protonated molecule, $[M+H]^+$. The MET ($C_{15}H_{25}NO_3$) has a molecular weight $[M+H]^+ = 268$. The information from the mass spectrum, such as observed mass, mass accuracy, retention time and empirical formula obtained by the equipment software used (LC/MSD TOF ESI-TOF), is shown in Tables S2–S5 (Supplementary material) for each scavenger studied.

The discussion on the intermediates formation and the main pathways involved in the MET degradation with TiO_2 doped 5% B (w/w) were investigated in a previous study [32] and can be summarized in hydroxylation of the benzene ring, shortening of methoxyl contained in the lateral chain, and cleavage or the addition of $HO^{\bullet}$ to the amine lateral chain. This section aims to compare the intermediates formed from MET degradation, in the presence of different scavengers, and propose a reaction path that follows MET in the absence of each active species evaluated.

Table 3 is a synopsis comparing the metoprolol's degradation products along the reaction time in the presence and/or absence of each scavenger. The structures proposed for the intermediaries formed are shown in Table S6 (Supplementary material).

Table 3
Products resulting from the photocatalytic degradation of MET observed by LC/MS using TiO_2 doped 5% B (w/w) in the presence and absence of scavengers.

Abbreviation*	Molecular formula	Scavengers				
		None	Air	BQ	t-BuOH	AF
CP-268	$C_{15}H_{25}NO_3$	√	√	√	√	√
CP-74	C_3H_7NO	–	√	–	–	–
CP-76	C_3H_9NO	–	√	–	–	–
CP-102	$C_5H_{11}NO$					√
CP-104	$C_5H_{13}NO$	–	–	–	√	
CP-113	$C_6H_8O_2$	–	–	–	√	
CP-116	$C_6H_{13}NO$	√	√	√	√	–
CP-118	$C_6H_{15}NO$	–	√	–	√	–
CP-120	$C_5H_{13}NO_2$	√	√	√	√	√
CP-129	$C_6H_{11}NO_2$	–	–	–	√	√
CP-134	$C_6H_{15}NO_2$	√	√	√	√	√
CP-141	$C_7H_8O_3$	–	√	–	–	–
CP-146	$C_6H_{11}NO_3$	–	–	–	–	√
CP-150	$C_6H_{15}NO_3$	√	√	√	√	–
CP-159	$C_8H_{14}O_3$	–	–	√	√	√
CP-176	$C_{10}H_9NO_2$	–	–	–	√	√
CP-200	$C_{10}H_{17}NO_3$	–	–	–	√	√
CP-220	$C_{13}H_{17}NO_2$	–	√	–	–	–
CP-226	$C_{12}H_{19}NO_3$	√	√	√	–	–
CP-231	$C_{11}H_{18}O_5$	–	√	–	–	–
CP-238	$C_{13}H_{19}NO_3$	√	√	√	√	√
CP-240	$C_{13}H_{21}NO_3$	√	√	√	√	–
CP-241	$C_{12}H_{16}O_5$	–	–	–	√	√
CP-252	$C_{14}H_{21}NO_3$	√	√	√	√	–
CP-254	$C_{14}H_{23}NO_3$	√	√	√	√	√
CP-256	$C_{13}H_{21}NO_4$	√	√	√	–	–
CP-259	$C_{12}H_{18}O_6$					√
CP-270	$C_{14}H_{23}NO_4$	√	√	√	√	–
CP-282	$C_{15}H_{23}NO_4$	√	√	√	√	–
CP-284	$C_{15}H_{25}NO_4$	√	√	√	√	√
CP-290	$C_{13}H_{23}NO_6$	–	√	–	√	–
CP-294	$C_{15}H_{19}NO_5$	–	–	–	√	–
CP-298	$C_{15}H_{23}NO_5$	√	√	√	–	–
CP-300	$C_{15}H_{25}NO_5$	√	√	√	√	–
CP-302	$C_{13}H_{19}NO_7$	–	–	–	√	–
CP-306	$C_{13}H_{23}NO_7$	–	√	–	–	–
CP-314	$C_{15}H_{23}NO_6$	–	–	–	√	–
CP-316	$C_{15}H_{25}NO_6$	√	√	√	√	–
CP-318	$C_{15}H_{27}NO_6$	√	√	√	–	–
CP-332	$C_{15}H_{25}NO_7$	–	√	√	–	–
CP-336	$C_{15}H_{29}NO_7$					√
CP-346	$C_{15}H_{23}NO_8$	–	√	–	–	–
CP-372	$C_{16}H_{15}NO_9$	–	–	–	√	–
CP-420	$C_{18}H_{29}NO_{10}$	–	√	–	–	–
CP-426	$C_{20}H_{27}NO_9$	–	–	√	–	–
CP-430	$C_{19}H_{27}NO_{10}$	–	–	–	√	–
CP-567	$C_{27}H_{38}N_2O_{11}$	–	–	–	√	–

Abbreviation* (in relation to m/z obtained).

3.2.1. Contribution of oxygen in the formation of the intermediates during reaction

With continuous air bubbling (air-saturated) in MET solution, it was observed a lot of intermediaries formed, which are in accordance with the obtained increase in degradation (76% removal of MET). A total of 28 products of MET degradation at m/z 74, m/z 76, m/z 116, m/z 118, m/z 120, m/z 134, m/z 141, m/z 150, m/z 220, m/z 226, m/z 231, m/z 238, m/z 240, m/z 252, m/z 254, m/z 256, m/z 270, m/z 282, m/z 284, m/z 290, m/z 298, m/z 300, m/z 306, m/z 316, m/z 318, m/z 332, m/z 346 and m/z 420 were detected. A mass spectrum

model with the formed intermediates at m/z 116, m/z 120, m/z 134 and m/z 150, in the presence of oxygen, is shown in Fig. S1 in the Supplementary material.

Many intermediaries appeared in the degraded solution only when air bubbling was used. Comparing the results of the degradation experiment with the catalyst alone and catalyst + oxygen, it appears that the intermediates of m/z 74, m/z 76, m/z 118, m/z 141, m/z 220, m/z 231, m/z 290, m/z 306, m/z 332, m/z 346 and m/z 420 were detected only in presence of oxygen.

These intermediates are formed due to a more advanced state of oxidation, increasing the rate of oxidation of the intermediate products and, consequently, obtaining the formation of a larger amount of intermediates resulting from the breach of the aliphatic part of the MET molecule, and of the hydroxylation in the aromatic ring corresponding to the attack of $O_2^{\bullet-}$ radicals [63]. Consequently, aromatic ring opening may occur via addition of hydroperoxyl radical/superoxide anion [64].

Intermediates resulting from the aliphatic part of the MET molecule were observed through fragments of the ethanolamine (m/z = 74, 76 and 118), probably due to the loss of the hydroxyl group and the loss of isopropyl moiety and/or the oxidation of the hydroxyl group [65].

The peak with m/z = 220 is a common fragmentation with the formation of aldehyde probably by reactions which involve attack on the ether functional group of the MET molecule side chain followed by elimination of water, thus generating a carbonyl, followed by an intermolecular electron transfer, generating a double bond [65].

The intermediates from the binding of HO$^{\bullet}$ radicals in the aromatic ring were detected: dihydroxylated intermediate with m/z 141, tetrahydroxylated intermediates with m/z = 332, 346 and 420.

The intermediate with m/z 141 was derivative of common fragment with m/z 240 (forming alcohol from attack in the ether functional group of the MET molecule). This intermediate was also identified by Romero et al. [66], but the author proposed a different structure.

The intermediate with m/z = 332 has already been identified as MET degradation intermediate [29,65,67]. Later the attack in the secondary amine moiety of intermediate with m/z 346 can occur, forming the intermediate with m/z = 420. At the best of our knowledge, no MET degradation intermediates of molecular mass 346 and 420 have been identified so far.

In our case though, the strong oxidative conditions lead to even more oxidized products, to which the aromatic ring has been opened (intermediates with m/z = 231, 290 and 306).

This is in agreement as mentioned in the literature, the $O_2^{\bullet-}$ radicals attack preferentially aromatic rings that suffering ring-opening reactions [21,48]. The intermediate with m/z = 290 also was identified by Veloutsou et al. [68], using photo-Fenton reaction, but the intermediates with m/z = 231 and m/z = 306 were not found in the literature.

The large number of intermediates (Table 2 and Table S2 in Supplementary material) identified in the degradation of MET by TiO$_2$ doped with 5% B (w/w) + oxygen shows how complex this kind of process can be and suggests a new MET photocatalytic degradation pathway in the presence of oxygen (Fig. 5).

3.2.2. By-products formed in MET degradation mainly by the participation of HO$^{\bullet}$ radicals and holes

During photocatalytic degradation of MET in the presence of BQ, a total of 20 intermediates were identified with m/z 116, m/z 120, m/z 134, m/z 150, m/z 159, m/z 226, m/z 238, m/z 240, m/z 252, m/z 254, m/z 256, m/z 270, m/z 282, m/z 284, m/z 298, m/z 300, m/z 316, m/z 318, m/z 332, and m/z 426 (Table 2 and Table S3 in Supplementary material). This process highlighted the formation of hydroxylated intermediates, corresponding to the attack of HO$^{\bullet}$ radicals on the aromatic ring of MET molecule resulted in the monohydroxylated derivative of MET (m/z = 284), different fragments of the monohydroxylated with m/z = 298, 270 and 256, dihydroxylated intermediates with m/z = 300, trihydroxylated intermediates with m/z = 316 and tetrahydroxylated intermediates with m/z = 332. Hydroxylated intermediates are common in MET degradation processes, as mentioned by other researchers [29,65–67,69].

The hydroxylation can lead to opening of the aromatic ring. The intermediate identified with m/z 159 shows the cleavage of the aromatic ring. This by-product was derivative of intermediate with m/z = 318, formed by cleavage of the aromatic ring combined with the hydroxylation of the secondary amine moiety. Another intermediate identified in the presence of BQ is the dimeric species at m/z = 426, that involves dimerization reactions of the species at m/z 300 and 316 probably involving direct reactions with holes. At the best of our knowledge, intermediates with m/z = 159 and 426, as presented in this work, were not found in the literature.

On the basis of the identified intermediates from MET degradation experiments in the presence of BQ, we propose a degradation pathway for MET photocatalytic degradation (using TiO$_2$/5% B (w/w) as catalyst) with predominance of HO$^{\bullet}$ radicals and holes (Fig. 6).

3.2.3. By-products formed in MET degradation mainly by the participation of $O_2^{\bullet-}$ radicals and holes

As observed in Fig. 3B the efficiency of the MET photodegradation decreases drastically when t-BuOH was added to the reaction system (80% of inhibition). However, in this case of decrease of the amount of HO$^{\bullet}$ radicals, a total of 28 products of MET degradation were detected with mass peaks at m/z 104, m/z 113, m/z 116, m/z 118, m/z 120, m/z 129, m/z 134, m/z 150, 159, m/zm/z 176, m/z 200, 238, m/zm/z 240, m/z 241, m/z 252, m/z 254, m/z 270, m/z 282, m/z 284, m/z 290, m/z 294, m/z 300, m/z 302, m/z 314, m/z 316, m/z 372, m/z 430 and m/z 567. This fact proves that the others active species (such as, $O_2^{\bullet-}$ radicals and holes) were also important in the degradation process.

In the presence of t-BuOH, preferably the $O_2^{\bullet-}$ radicals and positive holes by direct oxidation are available to attack the compound. The participation of $O_2^{\bullet-}$ has been reported to be involved in several oxidation mechanisms of organic compounds [21,48].

As mentioned previously, the $O_2^{\bullet-}$ radicals attack preferentially aromatic rings which undergo ring-opening reactions. The identified by-products, with mass peaks at m/z 113, m/z 129, m/z 159, m/z 200, m/z 241, m/z 290 and m/z 302, are characterized by the opening aromatic ring.

The intermediate with m/z 104 is the aliphatic part breakdown product of MET molecule.

After formation of the intermediate with m/z 238, the loss of water and isopropyl group generates the by-product with m/z 176.

The intermediate with m/z 294 could be formed by attack of $O_2^{\bullet-}$ radicals on the C atom next to the ether oxygen in the aliphatic part of intermediate with m/z 284, followed by oxidation of the hydroxyl group and the abstraction of hydrogen corresponding to isopropyl group.

The oxidation of the hydroxyl group of the aliphatic part of intermediate with m/z 316 generates the compound with m/z 314. After formation of this intermediate, it can occur the attack of $O_2^{\bullet-}$ radicals on the C atom next to the ether functional group followed by attack on the amino group. Kumar et al. [70] identified the degradation/interaction products formed in mixtures of atenolol (which is also a β-blocker) with a variety of pharmaceutical excipients. They proposed the most stable form of the attack on the amino group is by addition of —CO$_2$ group to form a carbamic acid, which was followed up by addition of —CO to yield a comparatively stable carbamic formic anhydride. From this attack, it is formed a compound

with m/z 402 (no identified) which subsequently generates the intermediate of m/z 372 and 430 by reactions involving attack on the ether side chain followed by addition of $-C_2H_4$ or elimination of $-CH_2O$ groups, respectively.

In this case, it was also observed the formation of a product resulting from dimerization reactions of the intermediates with m/z 300 and 316, generating the byproduct with m/z 567.

These intermediaries presented here (m/z 104, m/z 113, m/z 129, m/z 159, m/z 176, m/z 200, m/z 241, m/z 294, m/z 302, m/z 314, m/z 372 m/z 430 and m/z 567) were not detected by other researchers, except the intermediate with $m/z = 290$ which also was identified by Veloutsou et al. [68].

Based on these results, a possible photocatalytic degradation pathway of MET consisting of several steps was proposed in Fig. 7, considering the predominant contribution of $O_2^{\bullet-}$ radicals and holes.

3.2.4. By-products of MET degradation formed mainly by the participation of $O_2^{\bullet-}$ radicals

The decrease of the holes inhibits dramatically the reaction rate (as observed in Fig. 4B) because of the high activity of holes themselves and due to the inhibition of $HO^{\bullet}$ radicals formation. Since $HO^{\bullet}$ radicals and holes do not participate (or their participation is significantly decreased) in MET photocatalytic elimination, the reaction with $O_2^{\bullet-}$ radicals is favored in this system, which is a minor reaction pathway. Thus, only 13 degradation products were detected with mass peaks at m/z 102, m/z 120, m/z 134, m/z 146, m/z 159, m/z 176, m/z 200, m/z 238, m/z 241, m/z 254, m/z 259, m/z 284 and m/z 336. In this case, it highlights the presence of intermediates formed by ring-opening at m/z 159, m/z 200, m/z 241, m/z 259 and m/z 336. As discussed above (Section 3.2.1.), $O_2^{\bullet-}$ radicals attack preferentially the aromatic rings, which is in agreement with our results obtained. The intermediates with m/z 102 and 146 are fragments from side chain cleavage of the aliphatic part of MET molecule.

In comparison to other systems, the intermediates identified with m/z 102, 146, 259 and 336 were observed only in the presence of AF, and were not found in the literature.

By considering the identified intermediates, in Fig. 8 it is proposed a possible degradation pathway for MET, using TiO_2 doped with 5% B (w/w) with important contribution of $O_2^{\bullet-}$ radicals as active species.

3.2.5. Comparison of the results of each active species in MET degradation pathways

For a better comparison of the different proposed mechanisms during reaction on the effect of each active species investigated, a general MET degradation pathways have been proposed (Fig. 9) in the presence of different scavengers, based on data presented in Figs. 5–8. The results of scavenger experiments presented earlier clearly demonstrate distinct differences among the reaction mechanisms, especially in the presence of AF and t-BuOH, in which predominates reactions by way of $O_2^{\bullet-}$ radicals, leading to the formation of many intermediates resulting from the opening of the aromatic ring, as discussed above.

It is worth mentioning that the intermediates at m/z 120, m/z 134, m/z 238, m/z 254 and m/z 284 have been identified for all cases investigated (with different scavenger and non-scavenger systems). These are common degradation products of MET as mentioned by many researchers [29,32,65–69,71], whereas compounds at m/z 74, m/z 76, m/z 141, m/z 220, m/z 231, m/z 306, m/z 346, and m/z 420 were identified only in the presence of oxygen. Compounds at m/z 104, m/z 113, m/z 129, m/z 294, m/z 302, m/z 314, m/z 372, m/z 430 and m/z 567 were peculiarly identified only with t-BuOH, probably by reactions involving $O_2^{\bullet-}$ radicals and holes. In contrast, compounds at m/z 102, m/z 146, m/z 259, and m/z 336 were iden-

tified only with AF, probably by reactions involving $O_2^{\bullet-}$ radicals. Coherently, in the presence of BQ it was identified the intermediate at m/z 426 by reaction with holes.

4. Conclusions

Based on our experimental results in the presence of different scavengers of the active species ($HO^{\bullet}$, $O_2^{\bullet-}$ h_{VB}^+, e_{VC}^-), we summarize the most remarkable conclusions:

1. The oxidation of MET was primarily driven by participation of $HO^{\bullet}$, $O_2^{\bullet-}$ radicals and positive holes, using modified TiO_2 with 5% B as catalyst, and by $HO^{\bullet}$ radicals and holes using pure TiO_2, with much higher contribution of $HO^{\bullet}$ radicals on both catalysts. These differences in the contribution of active species in MET degradation (see Table 2) demonstrate that the generation of the active species depends on the properties of the catalyst, such as surface area, crystal phase, crystal size.

2. Oxygen plays an important role in the photocatalytic degradation of MET for both catalysts tested, because it is a scavenger of electrons with the formation of $O_2^{\bullet-}$ radicals, that lead to the decrease of e^-/h^+ pairs recombination and, consequently, leading to formation of more $HO^{\bullet}$ radicals.

3. From the byproducts formed, it can be observed that the $O_2^{\bullet-}$ radicals mostly attack the aromatic rings, leading to formation of compounds resulting from the opening of the aromatic ring. The $HO^{\bullet}$ radicals primarily leads to the formation of compounds mono-, di-, tri- and tetra-hydroxylated and their derivatives, and products formed by the loss of isopropyl portion. Finally, the direct attack by positive holes can lead to compounds resulting from dimerization products of MET molecule with high molecular weight.

Appendix A. Supplementary data

Supplementary data associated with this article can be found, in the online version, at http://dx.doi.org/10.1016/j.apcatb.2016. 04.054.

References

[1] M.I. Litter, Appl. Catal. B: Environ. 23 (1999) 89–114.
[2] M.A. Rauf, S.S. Ashraf, Chem. Eng. J. 151 (2009) 10–18.
[3] M.N. Chong, B. Jin, C.W.K. Chow, C. Saint, Water Res. 44 (2010) 2997–3027.
[4] N. De la Cruz, R.F. Dantas, J. Giménez, S. Esplugas, Appl. Catal. B: Environ. 130–131 (2013) 249–256.
[5] K. Kabra, R. Chaudhary, R.L. Sawhney, Ind. Eng. Chem. Res. 43 (2004) 7683–7696.
[6] S. Malato, P. Fernández-Ibáñez, M.I. Maldonado, J. Blanco, W. Gernjak, Catal. Today 147 (2009) 1–59.
[7] D.D. Ramos, P.C.S. Bezerra, F.H. Quina, R.F. Dantas, G.A. Casagrande, S.C. Oliveira, M.R.S. Oliveira, L.C.S. Oliveira, V.S. Ferreira, S.L. Oliveira, A. Machulek Jr., Environ. Sci. Pollut. Res. 22 (2015) 774–783.
[8] M.N. Abellán, J. Giménez, S. Esplugas, Catal. Today 144 (2009) 131–136.
[9] D. Chatterjee, S. Dasgupta, J. Photochem. Photobiol. C 6 (2005) 186–205.
[10] T.E. Doll, F.H. Frimmel, Water Res. 38 (2004) 955–964.

[11] A. Fujishima, X. Zhang, C. R. Chim. 9 (2006) 750–760.
[12] S.M. Gupta, M. Tripathi, Chin. Sci. Bull. 56 (2011) 1639–1657.
[13] R. Thiruvenkatachari, S. Vigneswaran, I.I.S. Moon, Korean J. Chem. Eng. 25 (2008) 64–72.
[14] M.R. Hoffmann, S.T. Martin, W. Choi, D.W. Bahnemann, Chem. Rev. 95 (1995) 69–96.
[15] M. Klavarioti, D. Mantzavinos, D. Kassinos, Environ. Int. 35 (2009) 402–417.
[16] B. Abramović, V. Despotović, D. Šojić, N. Finčur, React. Kinet. Mech. Catal. 115 (2015) 67–79.
[17] K. Nakata, A. Fujishima, J. Photochem. Photobiol. C 13 (2012) 169–189.
[18] L.M. Canle, J.A. Santaballa, E. Vulliet, J. Photochem. Photobiol. A: Chem. 175 (2005) 192–200.
[19] W. Wang, L. Zhang, T. An, G. Li, H.-Y. Yip, P.-K. Wong, Appl. Catal. B: Environ. 108–109 (2011) 108–116.
[20] Y. Chen, S. Yang, K. Wang, L. Lou, J. Photochem. Photobiol. A: Chem. 172 (2005) 47–54.
[21] R. Palominos, J. Freer, M.A. Mondaca, H.D. Mansilla, J. Photochem. Photobiol. A: Chem. 193 (2008) 139–145.
[22] X.V. Doorslaer, P.M. Heynderickx, K. Demeestere, K. Debevere, H.V. Langenhove, J. Dewulf, Appl. Catal. B: Environ. 111–112 (2012) 150–156.
[23] W. Li, D. Li, Y. Lin, P. Wang, W. Chen, X. Fu, Y. Shao, J. Phys. Chem. C 116 (2012) 3552–3560.
[24] L.M. Pastrana-Martínez, J.L. Faria, J.M. Doña-Rodríguez, C. Fernández-Rodríguez, A.M.T. Silva, Appl. Catal. B: Environ. 113–114 (2012) 221–227.
[25] H. Yang, G. Li, T. An, Y. Gao, J. Fu, Catal. Today 153 (2010) 200–207.
[26] R.P. Cavalcante, L.R. Sandim, D. Bogo, A.M.J. Barbosa, M.E. Osugi, M. Blanco, S.C. Oliveira, M.F.C. Matos, A. Machulek Jr., V.S. Ferreira, Environ. Sci. Pollut. Res. 20 (2013) 2352–2361.
[27] J. Rivera-Utrilla, M. Sánchez-Polo, M.Á. Ferro-García, G. Prados-Joya, R. Ocampo-Pérez, Chemosphere 93 (2013) 1268–1287.
[28] M.L. Wilde, S. Montipó, A.F. Martins, Water Res. 48 (2014) 280–295.
[29] B. Abramović, S. Kler, D. Sojić, M. Laušević, T. Radović, D. Vione, J. Hazard. Mater. 198 (2011) 123–132.
[30] A. Rubirola, M. Llorca, S. Rodriguez-Mozaz, N. Casas, I. Rodriguez-Roda, D. Barceló, G. Buttiglieri, Water Res. 63 (2014) 21–32.
[31] V. Romero, N. De la Cruz, R.F. Dantas, P. Marco, J. Giménez, S. Esplugas, Catal. Today 161 (2011) 115–120.
[32] R.P. Cavalcante, R.F. Dantas, H. Wender, B. Bayarri, O. González, J. Giménez, S. Esplugas, A. Machulek Jr., Appl. Catal. B: Environ. 176–177 (2015) 173–182.
[33] R.P. Cavalcante, R.F. Dantas, B. Bayarri, O. González, J. Giménez, S. Esplugas, A. Machulek Jr., Catal. Today 252 (2015) 27–34.
[34] W. Li, D. Li, J. Wang, Y. Shao, J. You, F. Teng, J. Mol. Catal. A-Chem. 380 (2013) 10–17.
[35] T. An, J. An, Y. Gao, G. Li, H. Fang, W. Song, Appl. Catal. B: Environ. 164 (2015) 279–287.
[36] N. De la Cruz, V. Romero, R.F. Dantas, P. Marco, B. Bayarri, J. Giménez, S. Esplugas, Catal. Today 209 (2013) 209–214.
[37] S. Ahmed, M.G. Rasul, R. Brown, M.A. Hashib, J. Environ. Manag. 92 (2011) 311–330.
[38] N. Mezioud, N. Bouziane, M.A. Malouki, A. Zertal, G. Mailhot, J. Photochem. Photobiol. A: Chem. 288 (2014) 13–22.
[39] N.K. Youn, J.E. Heo, O.S. Joo, H. Lee, J. Kim, B.K. Min, J. Hazard. Mater. 177 (2010) 216–221.
[40] S. Zheng, Y. Cai, K.E. O'shea, J. Photochem. Photobiol. A: Chem. 210 (2010) 61–68.
[41] N.A. Mir, A. Khan, M. Muneer, S. Vijayalakhsmi, Sci. Total Environ. 458–460 (2013) 388–398.
[42] D. Xia, T.W. Ng, T. An, G. Li, Y. Li, H.Y. Yip, H. Zhao, A. Lu, P.-K. Wong, Environ. Sci. Technol. 47 (2013) 11166–11173.
[43] R.A. Palominos, M.A. Mondaca, A. Giraldo, G. Peñuela, M. Pérez-Moya, H.D. Mansilla, Catal. Today 144 (2009) 100–105.
[44] S. Xu, J. Shen, S. Chen, M. Zhang, T. Shen, J. Photochem. Photobiol. B Biol. 67 (2002) 64–70.
[45] E.M. Rodríguez, G. Márquez, M. Tena, P.M. Álvarez, F.J. Beltrán, Appl. Catal. B: Environ. 178 (2015) 44–53.
[46] B.H.J. Bielski, D.E. Cabelli, R.L. Arudi, A.B. Ross, J. Phys. Chem. Ref. Data 14 (1985) 1041–1100.
[47] J. Bandara, J. Kiwi, N. J. Chem. 23 (1999) 717–724.
[48] P. Raja, A. Bozzi, H. Mansilla, J. Kiwi, J. Photochem. Photobiol. A: Chem. 169 (2005) 271–278.
[49] Y. Chen, A. Lu, Y. Li, L. Zhang, H.Y. Yip, H. Zhao, T. An, P.-K. Wong, Environ. Sci. Technol. 45 (2011) 5689–5695.
[50] H. Fang, Y. Gao, G. Li, J. An, P.-K. Wong, H. Fu, S. Yao, X. Nie, T. An, Environ. Sci. Technol. 47 (2013) 2704–2712.
[51] X. Zhang, D.D. Sun, G. Li, Y. Wang, J. Photochem. Photobiol. A: Chem. 199 (2008) 311–315.
[52] D. Zhang, R. Qiu, L. Song, B. Eric, Y. Mo, X. Huang, J. Hazard. Mater. 163 (2009) 843–847.
[53] R. Hazime, C. Ferronato, L. Fine, A. Salvador, F. Jaber, J.-M. Chovelon, Appl. Catal. B: Environ. 126 (2012) 90–99.
[54] M.S. Alam, B.S.M. Rao, E. Janata, Radiat. Phys. Chem. 67 (2003) 723–728.
[55] G.V. Buxton, C.L. Greenstock, W.P. Helman, A.B. Ross, J. Phys. Chem. Ref. Data 17 (1988) 513.
[56] Z. He, C. Wang, H. Wang, F. Hong, X. Xu, J. Chen, S. Song, J. Hazard. Mater. 189 (2011) 595–602.
[57] J. Ma, N.J.D. Graham, Water Res. 34 (2000) 3822–3828.
[58] K. Doudrick, T. Yang, K. Hristovski, P. Westerhoff, Appl. Catal. B: Environ. 136–137 (2013) 40–47.
[59] L.L. Perissinotti, M.A. Brusa, M.A. Grela, Langmuir 17 (2001) 8422–8427.
[60] S. Rengaraj, X.Z. Li, Chemosphere 66 (2007) 930–938.
[61] T. Tan, D. Beydoun, R. Amal, J. Photochem. Photobiol. A: Chem. 159 (2003) 273–280.
[62] M.N. Schuchmann, E. Bothe, J. von Sonntag, C. von Sonntag, J. Chem. Soc Perkin Trans. 2 (1998) 791–796.
[63] S. Canonica, U. Jans, K. Stemmler, J. Hoigné, Environ. Sci. Technol. 29 (1995) 1822–1831.
[64] D. Vialaton, C. Richard, Aquat. Sci. 64 (2002) 207–215.
[65] V. Romero, P. Marco, J. Giménez, S. Esplugas, Int. J. Photoenergy (2013), http://dx.doi.org/10.1155/2013/138918.
[66] V. Romero, F. Méndez-Arriaga, P. Marco, J. Giménez, S. Esplugas, Chem. Eng. J. 254 (2014) 17–29.
[67] H. Yang, T. An, G. Li, W. Song, W.J. Cooper, H. Luo, X. Guo, J. Hazard. Mater. 179 (2010) 834–839.
[68] S. Veloutsou, E. Bizani, K. Fytianos, Chemosphere 107 (2014) 180–186.
[69] Y. Yu, Y. Liu, X. Wu, Z. Weng, Y. Hou, L. Wu, Sep. Purif. Technol. 142 (2015) 1–7.
[70] V. Kumar, R.P. Shah, S. Malik, S. Singh, J. Pharm. Biomed. Anal. 49 (2009) 880–888.
[71] D. Šojić, V. Despotović, D. Orčić, E. Szabó, E. Arany, S. Armaković, E. Illés, K. Gajda-Schrantz, A. Dombi, T. Alapi, E. Sajben-Nagy, A. Palágyi, C. s. Vágvölgyi, L. Manczinger, L. Bjelica, B. Abramović, J. Hydrol. 472–473 (2012) 314–327.